Int. J. Chem. Sci.: 10(1), 2012, 479-489
ISSN 0972-768X
www.sadgurupublications.com

SYNTHESIS AND CHARACTERIZATION OF ELECTROLESS NANOCRYSTALLINE Ni-P ON ALUMINIUM

N. LATHA[a], V. RAJ[*], M. SELVAM[b] and P. MANISANKAR[c]

Advanced Materials Research Laboratory, Periyar University, SALEM – 636011 (T.N.) INDIA
[a]Department of Chemistry, Kandaswami Kandar's College,
PARAMATHI-VELUR – 638182 (T.N.) INDIA
[b]Central Electrochemical Research Institute, KARAIKUDI – 630006 (T.N.) INDIA
[c]Department of Industrial Chemistry, Alagappa University, KARAIKUDI – 630006 (T.N.) INDIA

ABSTRACT

A novel, convenient and cost effective method for synthesis of nanocrystalline nickel-phosphorus deposits were prepared by electroless deposition process on pre-treated aluminium from glycine bath. The samples were prepared by 80°C for 30 s, 600 s and 1800 s in acidic medium in the as-deposited condition. The nanocrystalline Ni-P surfaces were characterized by scanning electron microscopy, atomic force microscopy, energy dispersive X-ray analysis and X-ray diffraction methods. It was found that as-deposited Ni-P coatings formed in 30 s and 600 s were nanocrystalline and they were transformed into amorphous in the coating formed at 1800 s in the deposited condition.

Key words: Electroless deposition, Nanocrystalline Ni-P, SEM, AFM, XRD.

INTRODUCTION

Aluminum is an important material of research because it is widely used in industrial applications especially in aerospace, automotive, electrical, mechanical, household and computer industries. It has light weight, high electrical capacity, high energy density and low price. It has a nature of prone to corrosion in seawater and it requires specific surface preparation for successful deposition[1-5]. It is covered with a thin oxide layer on the surface. Hence, it is difficult to deposit any metal on aluminium with relatively good adhesion. There are different routes to enhance the corrosion resistance of aluminium alloys. Zincating is one of the most important methods for pretreatment of aluminium, which is widely used in the industry. The zincating process usually consists of double immersion into the zincate bath to form uniform coating of zinc on the aluminium surface[6-8]. Techniques such as physical

[*]Author for correspondence; E-mail: alaguraj2@rediffmail.com

vapour deposition, chemical vapour deposition, laser ablation, sputtering, electrodeposition and electroless deposition have been proposed to synthesize Ni-P coating. Among them, electroless nickel plating is the one of the most favorable method for the synthesis of nanocrystalline metal due to its advantages of low working cost, good controllability, high corrosion resistance and uniform coating in complex parts[9-15]. The nanocrystalline materials differ significantly than those of bulk materials due to its small size and high surface to bulk ratio. Nanomaterials are coated on various base materials such as, alumina, carbon, polymers etc. for their improved catalytic applications[16,17].

Material properties of electroless deposit greatly depend on the phosphorus content. According to the content of phosphorus, the electroless Ni–P can be classified into three categories as low, medium, and high phosphorus in the as-deposited state. Low-phosphorus deposit may consist of crystalline phase. The high phosphorus deposit may be either fully amorphous/nanocrystalline or mixture of amorphous and microcrystalline nickel phase. The medium phosphorus deposits might be similar to high phosphorus deposits[18-22].

In the present paper, we have prepared a nanocrystalline Ni-P coating with different contents of phosphorus obtained by changing the time of electroless deposition process. The aim of this present study is to provide a satisfactory investigation for the synthesis and characterization of nanocrystalline Ni-P coating on aluminium from glycine bath.

EXPERIMENTAL

Electroless nickel-phosphorus plating

Aluminium plates (7 x 1 x 0.1 cm) were used as the substrate for Ni-P electroless plating. The substrates were degreased with acetone, alkaline cleaned with 5% (w/v) sodium hydroxide, acid cleaning with 20% (v/v) HNO_3 and zincated before electroless plating. The electroless bath consist of nickel sulphate 42 g/L, glycine 11 g/L and sodium hypophosphite 21 g/L were used as the nickel ion source, complexing agent and reducing agent, respectively.

Coating characterizations

The nanocrystalline Ni-P coatings on aluminium were analysed by scanning electron microscope, SEM (JEOL-Japan-JSM-840A) and the elemental compositions of the deposits were determined with an energy dispersive X-ray analysis. (EDAX, Oxford link ISIS 300). The surface topography of the Ni–P deposits was analyzed by atomic force microscopy (AFM) (Digital Instruments CP-II Veeco Company, USA). The crystallographic structure and grain size of the Ni–P deposit coating was determined from a Philips X'pert X-ray diffractometer with Cu Kα radiation.

RESULTS AND DISCUSSION

EDAX analysis

The electroless nickel is deposited by an autocatalytic chemical reaction between the zincated aluminium surface and plating solution. The overall chemical reaction can be represented as follows

$$2\,[H_2PO_2]^- + Ni^{2+} + H_2O \rightarrow [HPO_3]^{2-} + Ni^o + P + 1/2\,H_2 \uparrow + 2\,H_2O \quad \ldots(1)$$

The compositions of the electroless deposits were measured by using EDAX. Fig. 1 shows the effect of plating time on at.% P and Ni in the coatings. When the plating time is increased from 30 s to 1800 s, at.% P decreases to some extent, which might be due to less H^+ ions. Furthermore, there was an increase in at % Ni.

$$2\,H_{ad} \longrightarrow H_2 \quad \ldots(2)$$

EDAX spectra of electroless Ni-P coatings formed in 30 s and 1800 s are shown in Fig. 2 (a, b). An EDAX spectrum at 30 s deposition time shows Ni and P peak and small amount of zinc is also present. The zinc peak comes from the zincating bath. At 1800 s deposition time, EDAX spectra shows Ni and P peak only. If the coating time increases, the zinc peak disappears. From the spectra, the presence of Ni and P is evident in the as-deposited coating.

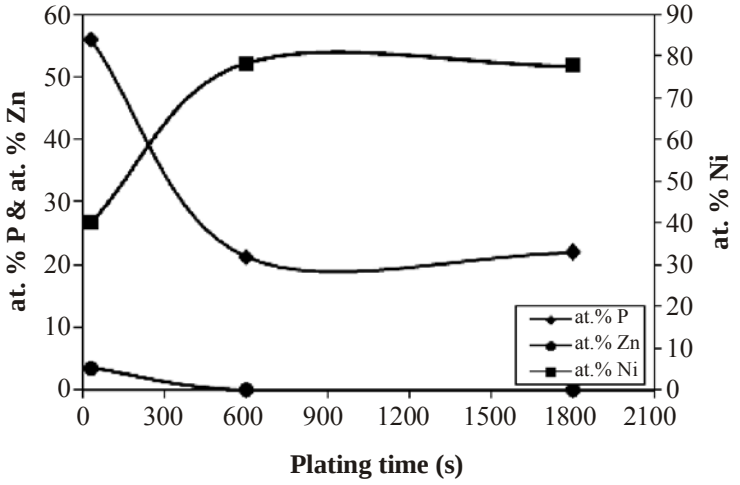

Fig. 1: Effect of plating time on atomic % of phosphorus and nickel

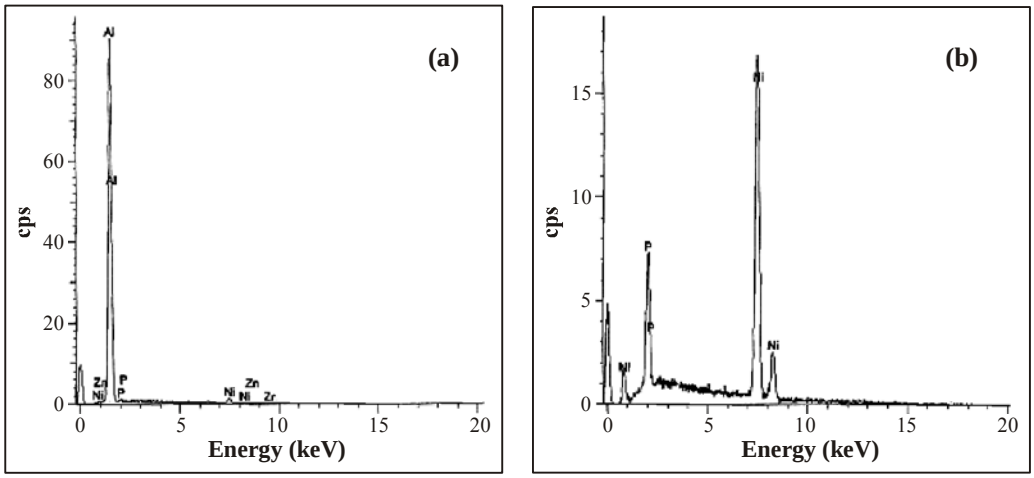

Fig. 2: EDAX spectra of electroless nickel phosphorus on zincated aluminium at various depositions time (a) 30 s and (b) 1800 s

Surface analysis by SEM

SEM images of the as-deposited electroless Ni-P obtained at 30 s, 600 s and 1800 s are given in Fig. 3 (a, b), (c, d) and (e, f) respectively in two magnifications X 3,000 and X 40,000. The surface structure of as-deposited Ni-P deposit produced at 30 s shows homogeneous structure as shown in Fig. 3 (a, b). Nickel deposition starts to develop by nucleation after dissolution of the zincated aluminium substrate. SEM images in Fig. 3 (c, d), (e, f) after 600 s and 1800 s of electroless deposition show a significant change on the Al surface. Ni-P deposits formed at 600 s of the as-deposited plate have tiny spherical nodular structure and formation of more uniform crystal structure as shown in Fig. 3 (c, d). The surface morphology of Ni-P deposits produced at 1800 s has smaller crystals with increased dimension and the larger number of nodular grains, fully covered on the surface of aluminium without any pores as shown in Fig. 3 (e, f). The deposits have matt bright finish at 30 s depositions, and very shiny smooth surface at 600 s and 1800 s deposition.

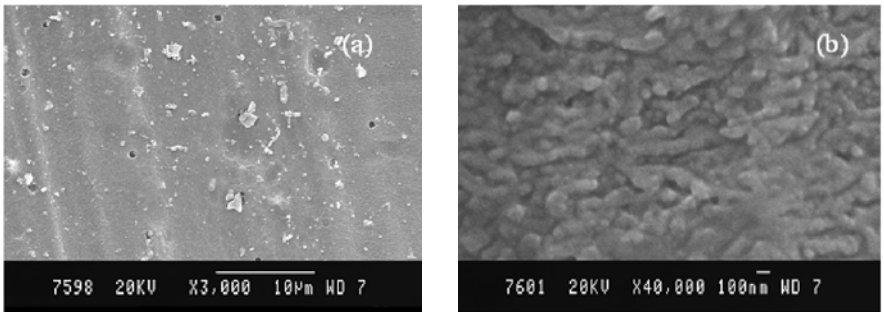

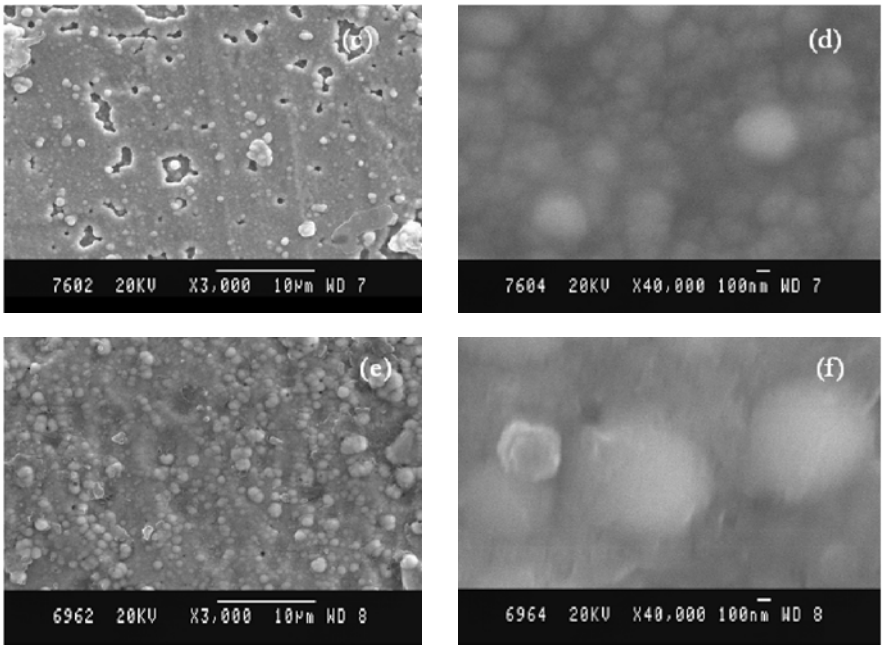

Fig. 3: SEM images of electroless nickel on zincated aluminium in the as-deposited state in two magnifications of X3, 000, X40, 000 (a, b) 30 s, (c, d) 600 s and (e, f) 1800 s

Surface analysis by AFM

Fig. 4 (a-c) and Fig. 5 (a-c) show the AFM images of (a) surface topographic view (2D) (b) three - dimensional view (3D) and (c) depth profile of electroless Ni-P coatings deposited on zincated aluminium at 30 s and 1800 s, respectively. According to the AFM picture, surface morphology of the electroless nickel coating is characterized at relatively short times. The deposits formed have nodular spherical grains with uniform size (Fig. 4 (a, b)). The depth profile analysis in the horizontal direction (Fig. 4c) shows smaller peaks in the measured surface area of 2 μm x 2 μm. The width of a peak distance is measured along the 'X' axis and gives the size of the particular crystal. The crystal size is in the range of less than 100 nm.

The AFM images in Fig. 5 (a, b) reveal that in the coating formed at 1800 s deposition time, the growing Ni-P crystals overlap and form larger nodular structure with uniform morphology. The depth profile analysis in the horizontal direction (Fig. 5c) shows broader peaks in the measured surface area of 4 μm X 4 μm. No sharp peaks are found, i.e. the coating is amorphous in nature. The size of the grain is less than 250 nm.

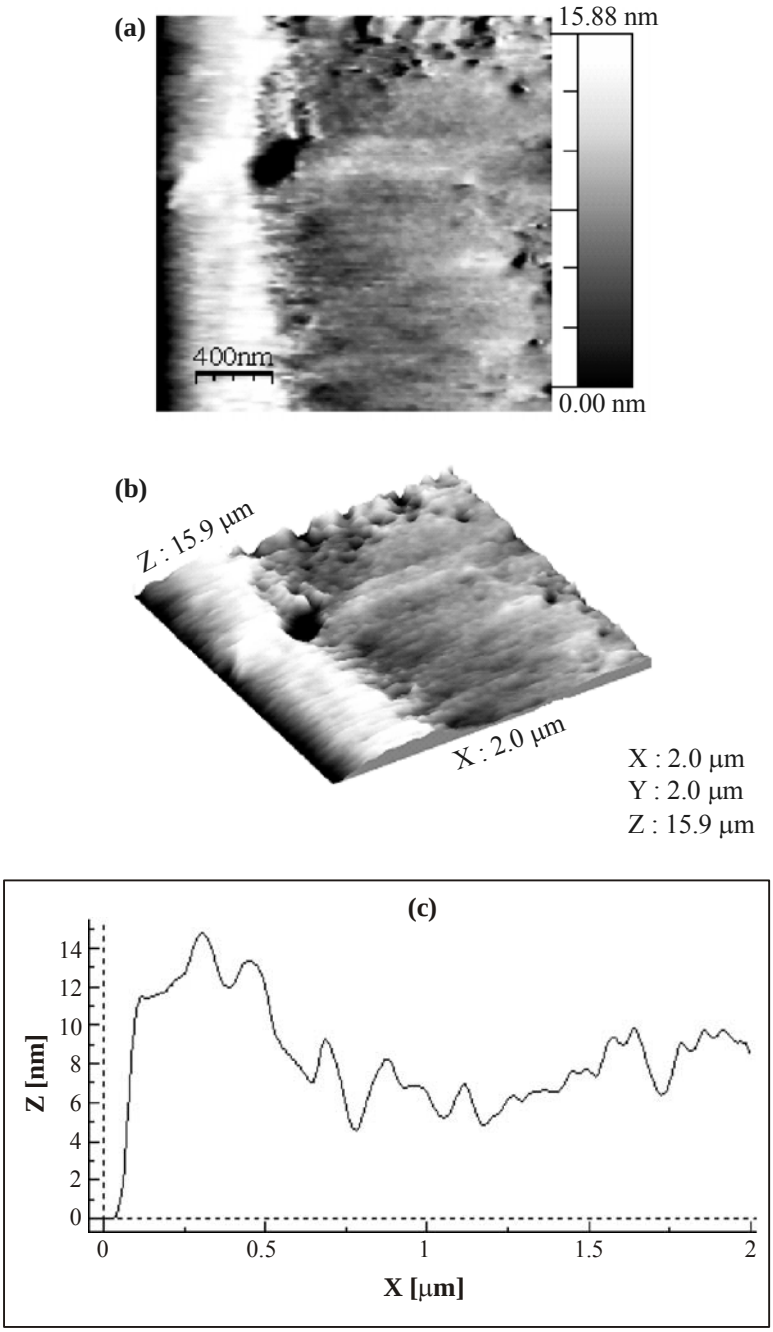

Fig. 4: AFM images of as-deposited electroless Ni-P (30 s) coating on zincated aluminium (a) Topographic image (b) 3-Dimensional and (c) Depth profile analysis image

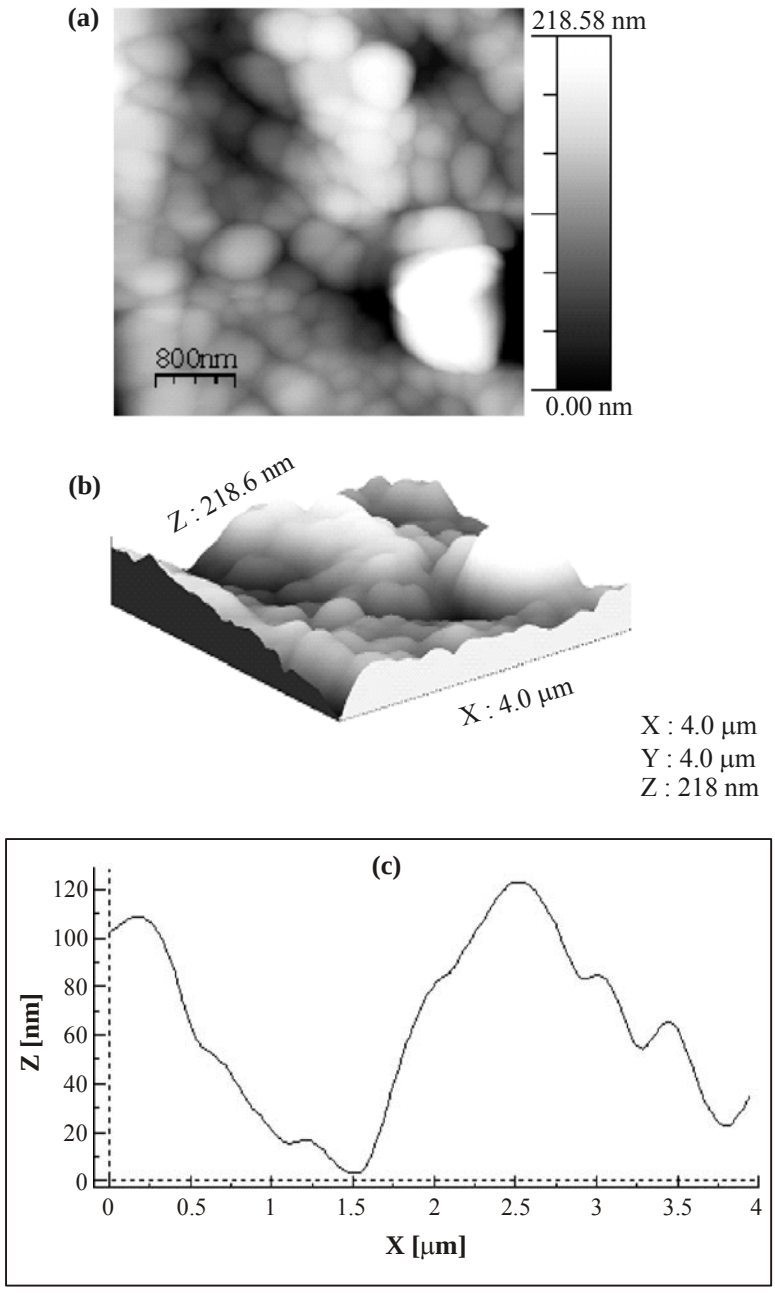

Fig. 5: AFM images of as-deposited electroless Ni-P (1800 s) coating on zincated aluminium (a) Topographic image (b) 3-Dimensional (c) Depth profile analysis

The average surface roughness (Ra) of the as-deposited electroless NC-Ni-P coatings on zincated aluminium according to the AFM measurements is 38.7 nm for 30 s deposition time and 19.9 nm for 1800 s deposition time and the corresponding RMS values are 54.4 nm and 24.4 nm respectively. As the deposition time increases, roughness decreases, because of the increase in smoothness of the coating.

X-ray diffraction analysis

Fig. 6 (a-c) shows X-ray diffraction patterns of electroless Ni-P on aluminium obtained from optimized electroless bath at various deposition times of 30 s, 600 s and 1800 s, respectively. It is seen from the Fig. 6 (a, b) that sharp peaks appear around 38°, 44°, 65° and 78° corresponding to P (1 1 8) (JCPDS No. 75-0577), Ni (1 1 1) (JCPDS No. 03-1051), P (0 2 3) (JCPDS No. 65-2491) and Ni (2 2 0) (JCPDS No. 88-2326) after 30 s and 600 s

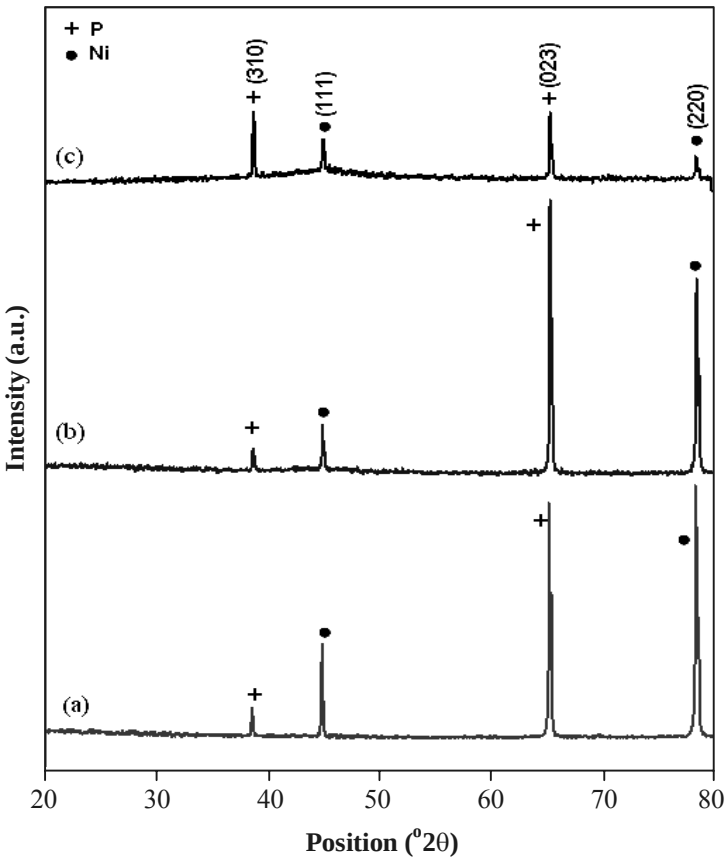

Fig. 6: XRD patterns of the electroless nickel phosphorus on zincated aluminium (a) 30 s; (b) 600 s; (c) 1800 s

deposition time. The peak shows discrete (h k l) reflections corresponding to face centered cubic and other structures. These results suggest that crystal planes observed in these textures are grown parallel to the aluminium substrate textures. From Fig. 6(c), for 1800 s deposition time, different textures are developed, such as P (3 1 0) (JCPDS No. 02-0266) appears at 38.85^o, Ni (1 1 1) at 45.09^o (JCPDS No. 01-1266), P (0 2 3) at 65.42 (JCPDS No. 65-2491) and Ni (2 2 0) (JCPDS No. 88-2326). The XRD pattern reveals broad peak at 2θ value of 40-50^o, indicating that the nickel-phosphorous alloys are amorphous in nature. It has been widely observed that fresh bath deposits have fine crystalline structures but deviation from crystallinity increase with increase in time and thickness. The sharp peak is obtained from the (1 1 1) diffraction of nanocrystalline Ni and the broad peak is obtained from the diffraction of amorphous phase or nanocrystalline phase in the electroless nickel deposit. This implies that the structure of the Ni–P deposit is different, even though the content of phosphorus is nearly equal. The surface structure is affected by process parameters, such as plating time, pH value, bathing temperature and complexing agents[23]. From these results, Ni-P deposits containing amorphous/nanocrystalline phase by adjusting the process parameters.

From 2θ and FWHM values, the crystal size of the Ni-P deposits were calculated using Scherrer's equation[24] $D = 0.9\lambda / \beta\cos\theta$, where λ is the radiation wavelength, β is the full width at half maximum (FWHM) and θ is the diffraction angle of the main peak. The average calculated crystal size is 81.4 nm, 76.9 nm and 49.7 nm for the deposition time of 30 s, 600 s and 1800 s respectively. In the coating formed at the deposition time of 1800 s, the amorphous structure is found.

CONCLUSION

This is the first report, where nickel phosphorus nanocrystals with grain sizes less than 100 nm were synthesized by electroless method from glycine bath. XRD, EDAX, SEM and AFM, results revealed their structure, composition and morphology. We believe that this method can open a new avenue for deposition of metallic nanostructures based on aluminium substrates for desired properties. It proves itself to be a cost-effective, high efficiency method in future application of aerospace, industrial and automotive.

ACKNOWLEDGMENT

One of the authors (N. Latha) gratefully acknowledges the University Grants Commission, New Delhi, India for financial assistance under the Minor Research Project Scheme (Project No. MRP 3162/09) and Dr. Gurulinga (IISc, Bangalore) for help in SEM studies.

REFERENCES

1. A. M. Addel-Gaber, B. A. Abd-El-Nabey and I. M. Sidahmed, Mater. Chem and Phys., **98**, 291 (2006).
2. A. K. Sharma, A. Rajendra and R. L. Gayathri, Alum. Trans., **1**, 155 (1999).
3. H. Jha, T. Kikuchi, M. Sakairi and H. Takahashi, Mater. Lett., **63**, 1451 (2009).
4. E. A. Starke, Jr. and J. T. Staley. Prog. Aerosp. Sci., **32**, 131 (1995).
5. A. K. Mukhopadhyay and A. K. Sharma. Surf. Coat. Technol., **92**, 212 (1997)
6. F. A. Lowenheim, Modern Electroplating, Third Edition, J. Wiley and Sons, Inc., NY, (1974)
7. G. O. Mallory, Plat. Surf. Finish, **72,** 6 (1985).
8. K. Azumi, T. Yugiri, T. Kurihara, M. Seo, H. Habazaki and S. Fujimoto, J. Electrochem. Soc., **C461**, 150 (2003).
9. G. O. Mallory and J. B. Hajdu, Editors, Electroless Plating: Fundamentals and Applications, Orlando: American Electropletters and Surface Finishers Society, (1990).
10. A. Brenner, E. G. Couch and E. K. Williams. J. Res. NBS., **44**, 109 (1950).
11. C. H. De Minjer and A. Brenner, Plating, **44**, 1297 (1957).
12. H. Yan, New Techniques in Electroless Nickel and Composite Plating, Industry of National Defense Press, Beijing, (2001).
13. A. Brenner and G. Riddel, J. Res. Natl. Bur. Stand., **37**, 31 (1946).
14. W. Riedel, Electroless Nickel Plating, ASM International/Finishing Publications, (1991).
15. M. Crobu, A. Scorciapino, B. Elsener and A. Rossi, J. Electrochim. Acta., **53,** 3364 (2008)
16. K. G. Keong, W. Sha and S. Malinov, J. Alloys Comp., **334**, 192 (2002).
17. C. Luo, Y. Zhang and Y. Wang, J. Mol. Catal A; Chem., **229**, 7 (2005).
18. H. S. Yu, S. F. Luo and Y. R. Wang, Surf. Coat. Technol., **148**, 143 (2001).
19. T. H. Hentschel, D. Isheim, R. Kirchheim, F. Muller and H. Kreye, Acta Mater., **48**, 933 (2000).

20. K. G. Keong, W. Sha and S. Malinov, J. Mater. Sci., **37**, 4445 (2002).

21. T. S. N. Sankara Narayanan, I. Baskaran, K. Krishnaveni and S. Parthiban, Surf. Coat. Technol., **200**, 3438 (2006).

22. G. Cao, Nanostructures & Nanomaterials: Synthesis, Properties & Applications, 1st Ed. Imperial College Press, Danvers (2004).

23. Y. H. Cheng, Y. Zou, L. Cheng and W. Liu, Mater. Sci. Technol., **24**, 457 (2008).

24. M. Mubarak Ali and V. Raj, J. Appl. Surf. Sci., **256**, 3841 (2010).

Accepted : 27.10.2011